PORTIONS OF THIS DOCUMENT ARE ILLEGIBLE

BLANK PAGE

LA-UR -7[illegible]

MASTER

TITLE:

LIGHT SCATTERING WITH STREAM-IN-AIR FLOW SYSTEMS

AUTHOR(S):

[illegible] S[illegible]man and M. J. [illegible]

SUBMITTED TO:

In: Proceedings of the Sixth Engineering Foundation Conference on Automated Cytology, Elmau, West Germany (April [illegible]-29, 197[illegible]), Brian H. Mayall, Ed. (Journal of Histochemistry and Cytochemistry)

los alamos
scientific laboratory
of the University of California
LOS ALAMOS, NEW MEXICO 87545

Running title: Stream-in-Air Flow Systems

LIGHT SCATTERING WITH STREAM-IN-AIR FLOW SYSTEMS

G. C. Salzman and M. E. Wilder

Biophysics and Instrumentation Group, Los Alamos

Scientific Laboratory, University of California

Los Alamos, New Mexico 87545

Received for publication ________________________, 1978

Send proofs to: Dr. G. C. Salzman
Biophysics and Instrumentation Group (MS888)
Los Alamos Scientific Laboratory
University of California
Los Alamos, New Mexico 87545

SUMMARY

Both forward angle and 90° light-scattering measurements have been used for cell sizing with stream-in-air flow systems with very little theoretical base for the measurements. Mie theory calculations are compared with measurements on plastic microspheres. Detector response for homogeneous spheres is shown to be sensitive to refractive index, as well as to particle position within the cell stream.

Stream-in-air flow systems based on the original Stanford design (1,3) have become increasingly popular in recent years, particularly since the systems became commercially available (2,4). Both forward angle and 90° light scattering have been used with these systems for cell sizing with the assumption that the scattered light intensity increases monotonically with cell size. In this paper, we compare exact electromagnetic theory calculations for the scatter sensors used in the two commercially available cell sorters with measurements on plastic microspheres. We also present calculations showing the effects on scattered light intensity of changes in particle refractive index and particle position within the cell stream.

MATERIALS AND METHODS

In the stream-in-air flow chamber, the sample stream is surrounded by a cell-free sheath fluid and passes vertically downward through a 50- to 100-μm diameter orifice and through a focused laser beam lying in the horizontal plane a few millimeters below the orifice. Since the cylindrical stream strongly refracts and reflects the laser beam, the light collection lenses in the scatter detectors have horizontal beam stops that block the light scattered at small angles relative to the horizontal plane.

A typical forward scatter detector geometry is shown in Fig. 1 from the viewpoint of detector space. The angles θ_2 and ϕ_2 in detector space are those which would be measured if the cell stream consisted of air instead of water. H is the vertical height of the beam stop, and R_{max} is the effective radius of the scattered light collection lens. This radius is generally somewhat less than the full lens radius and depends on iris settings and lens mounting conditions. D (θ_2, ϕ_2) is a small element on the face of the collection lens. The detector response is determined by integrating the response at D over the exposed face of the lens. Figure 2 shows the scattering geometry in cell space inside the stream. The center of the stream is at O, the laser beam is collinear with the z axis, the cell or particle is located at an arbitrary point, C, and the scattered light ray intersects the stream surface at S. The true scattering angles which are used in the electromagnetic theory scattering calculations are θ_1 and ϕ_1. These angles depend on θ_2 and ϕ_2 but are, in general, numerically different.

For every point D (θ_2, ϕ_2) in an array on the detector face, internal angles, θ_1 and ϕ_1, are calculated using a non-linear least squares minimization code which implements the Levenberg-Marquardt algorithm (7,8). The scattered light intensity in the direction (θ_1, ϕ_1) for a homogeneous spherical particle located at C is then calculated using exact electromagnetic theory (5,11), often referred to as Mie theory (9). The array of points, D (θ_2, ϕ_2), consists of 20 uniformly spaced values for θ_2 and nine uniformly spaced values for ϕ_2 in the upper half plane. The calculated intensities are then averaged to give the detector response. The calculations and measurements presented are for two commercially available stream-in-air flow systems: the Becton-Dickinson FACS-II (1) and a prototype of the Coulter TPS-1 (4). In all cases, the particle volume is assumed to be uniformly illuminated at 488 nm. Imposition of a Gaussian laser beam profile will enhance the cell position effects described below.

RESULTS

Table I gives the pertinent dimensions used in the calculations. Figure 3 shows the detector response vs particle diameter as a function of particle relative refractive index for the forward scatter detectors in these two systems. The experimental data points are for plastic microspheres whose characteristics are given in Table II. The imaginary component of the refractive index was assumed to be 0.0 for all the calculations shown in the figures. The relative refractive index m = 1.0 corresponds to a homogeneous sphere model for a live cell, m = 1.12 to that for a fixed cell, and m = 1.20 to that for a polystyrene latex sphere immersed in a saline solution whose refractive index is 1.3345. The mismatch between theory and experiment for the 15.7- and 18-μm diameter spheres is considered in the discussion section. Note that the response is rather flat in the diameter region below 5 μm, implying that one would obtain very small light-scatter coefficients of variation for small particles with significant volume coefficients of variation. Note also that the FACS-II system is more sensitive to particle refractive index changes than is the TPS-1 system.

The forward scatter detector response is affected by the position of the particle within the stream. Figure 4 shows the calculated effects of particle position on the detector response vs particle diameter curves for the two systems for two different particle relative refractive indices. The figure legends give the coordinates of the particle center (X_C, Y_C, Z_C) in μm with respect to the center of the sample stream. These effects are illustrated more dramatically in Fig. 5 which shows a comparison between experimental and calculated scatter intensity frequency histograms for 10-μm diameter polystyrene latex microspheres (10). The calculated distributions were obtained by Monte Carlo methods using the experimental Coulter volume distributions and the calculated position distributions. The Coulter volume frequency histogram was transformed into a diameter distribution and divided into five bins with appropriately assigned probabilities. A two-dimensional map of detector response vs particle position was generated for each diameter bin, and then an appropriate number of particles was selected at random from a normal distribution (6) with the standard deviations noted in the figure legend. The model data with 0.1-μm standard deviation reflect the particle size distribution. Only 4000 particles were used to generate this distribution to maintain a reasonable scale on the graph. The σ = 0.75-μm calculations and the experimental data both contain 19,166 points.

The effects of refractive index on the 90° scatter detector response function for the FACS-II are shown in Fig. 6. The particles are assumed to be centered in the cell stream. Note that the refractive index dependence is now inverted with respect to that of the forward scatter detector. The mismatch between theory and experiment at the 15.7- and 18-μm diameters is discussed below. Figure 7 shows the effects of cell position on the 90° scatter detector response function. Particle coordinates (X_C, Y_C, Z_C) inside the cell stream are given in the figure legend.

DISCUSSION

Since the 15.7- and 18-μm diameter spheres were darkly colored, imaginary refractive indices were chosen to minimize simultaneously the discrepancies between theory and experiment for each of these two particle sizes for the data in Figs. 3A and 3B and Fig. 6. An imaginary refractive index, n_i, of 0.0015 was successful in moving the calculation for the 18-μm diameter spheres to within one standard deviation of the experimental data for all three detectors. An n_i value of 0.0009 moved the calculations for the 15.7-μm diameter spheres to within 1.6 standard deviations for the FACS-II and TPS-1 forward scatter detectors. However, this correction still left the calculation for the 90° FACS-II detector seven standard deviations above the experimental data.

It has been shown that the response of scattered light detectors for two commercial stream-in-air cell sorters is sensitive both to particle refractive index and position within the stream. The effects of cell position within the sample stream can be minimized by using a concentrated sample and adjusting the sheath and sample pressures so that the sample stream diameter within the sheath stream is minimized. To address the effects of refractive index changes and non-monoticity of the scatter detector response function, care should be taken in interpreting the data when, for example, comparing frequency histograms of cells prepared with different fixatives. Although these results are strictly applicable only to homogeneous spheres, they shed some light on problems likely to be encountered with biological cells.

[illegible]

The authors would especially like to thank [illegible] and [illegible] Wund rlich of the Immunology Branch, National Cancer Institute, for providing the FACS-II data. We would also like to thank [illegible] and M. [illegible] for [illegible] Mrs. Elizabeth Sullivan for preparing the [illegible] photographs.

This work was performed under the auspices of the United States Department of Energy and was partially supported by the [illegible] of the National Cancer Institute [illegible].

[illegible]

1. Arndt-Jovin DJ, Jovin TM: Computer-controlled multiparameter analysis and sorting of cells and particles. J Histochem Cytochem 22:622 (1974)
2. Becton-Dickinson Electronics Laboratory, 506 Clyde Avenue, Mountain View, California 94043
3. [illegible] sorting. Rev Sci Instrum [illegible]
4. Coulter Electronics, Inc., 590 West 20th Street, Hialeah, Florida 33010
5. Dave JV: Subroutine for Computing the Parameters of the Electromagnetic Radiation Scattered by a Sphere. International Business Machines Scientific Center, Palo Alto, California, report [illegible] (May 1968)
6. Kinderman AJ, Ramage JG: Computer generation of normal random variables. J Am Stat Assoc 71:893 (1976)
7. [illegible]: A method for the solution of certain non-linear problems in least squares. Quart Appl Math 2:164 (1944)
8. Marquardt DW: An algorithm for least squares estimation of nonlinear parameters. SIAM J Appl Math 11:431 (1963)
9. Mie G: Beitraege zur Optik trueber Medien speziell kolloidaler Metalloesungen. Ann Physik 25:377 (1908)
10. Particle Technology, Inc., Los Alamos, New Mexico 87544 (now a subsidiary of Coulter Electronics, Inc., Hialeah, Florida 33010)
11. Stratton JA: Electromagnetic Theory. McGraw-Hill Company, New York, 19[illegible]

TABLE I

Detector Geometry Specifications Used in the Calculations

Parameter	FACS-II Forward	FACS-II 90°	TPC-[illegible]
H (mm)	1.45	0.56	2.6
R_{max} (mm)	6	3.9	10.5
Z_D (mm)	22	--	25.4
s (μm)	30	30	38.1
Y_D (mm)	--	5.2	--

TABLE II

[illegible] [a]

[illegible]	[illegible]	[illegible]	[illegible] coefficient
5.0	11	Cl[illegible]	[illegible]
7.9	1[illegible]	Clear	5.[illegible]
10.0	40[illegible]	Pale ora[illegible]	[illegible]
1[illegible].7	[illegible]	Dark [illegible]	[illegible]
18.0	2[illegible]	Dark re[illegible]	[illegible]

[a] [illegible] wavelength [illegible] nm.

FIG. 1. Scattering geometry as viewed from the detector space when refractive effects due to cylindrical geometry are ignored. The scattering angles θ_2 and ϕ_2 are calculated as if the cell stream were composed of air. R_{max} is the radius of the largest circle on the light collection lens such that all light passing through the circle reaches the photodetector. H is the [illegible] of the beam stop, and D (θ_2, ϕ_2) is an element of area on the face of the collection lens.

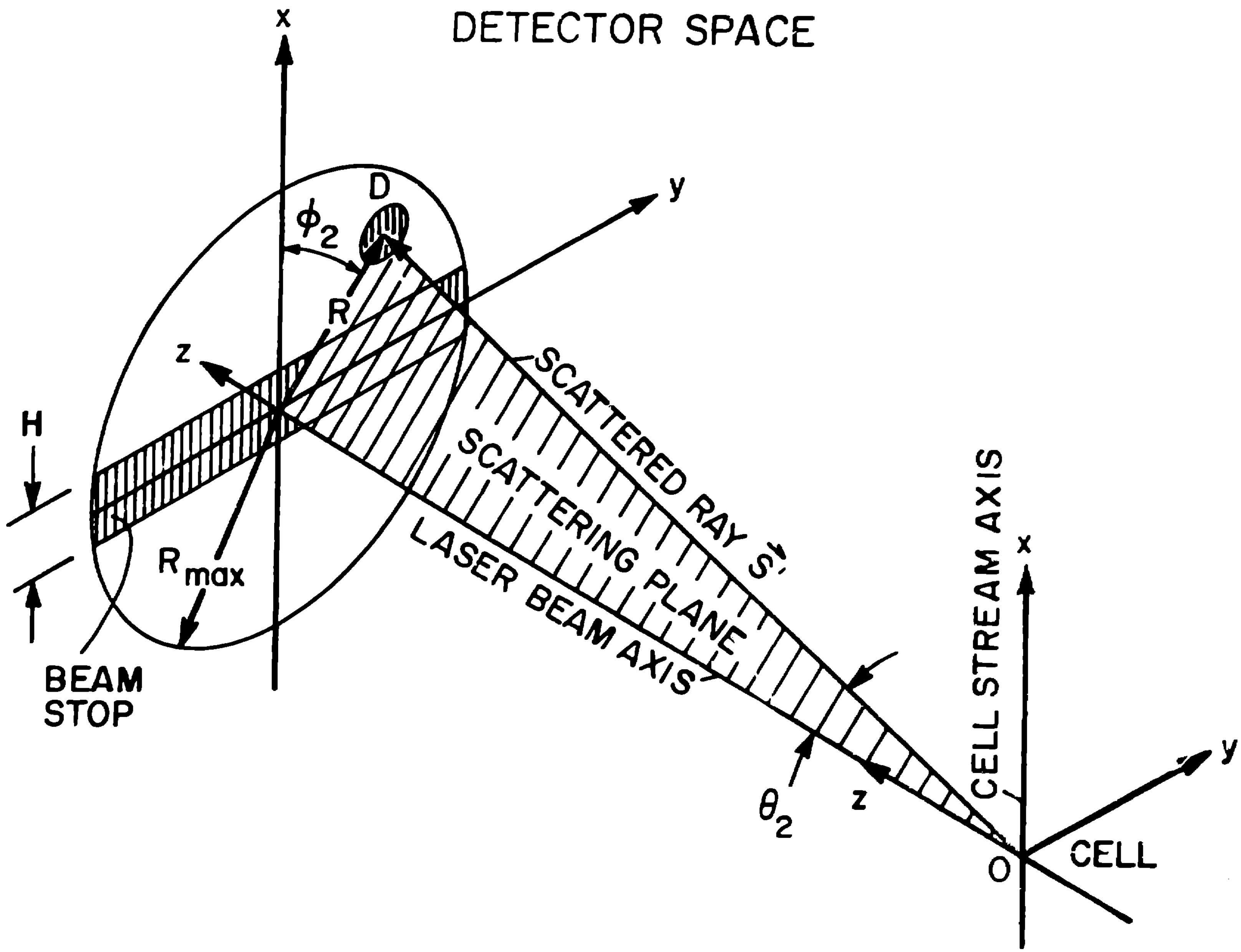
DETECTOR SPACE
x
y
z
D
ϕ_2
R
H
R_{max}
BEAM STOP
SCATTERED RAY $\vec{S}_1$
SCATTERING PLANE
LASER BEAM AXIS
θ_2
z
CELL STREAM AXIS
x
y
O
CELL

FIG. 2. Scattering geometry as viewed from the cell space inside the saline stream. The center of the stream is at O, and the cell or particle is centered at an arbitrary point C. A scattered light ray at C is refracted at the stream boundary, S, to reach the detector at D. The internal scattering angles θ_1 and ϕ_1 depend on θ_2 and ϕ_2 in a non-linear fashion. The stream radius is [illegible].

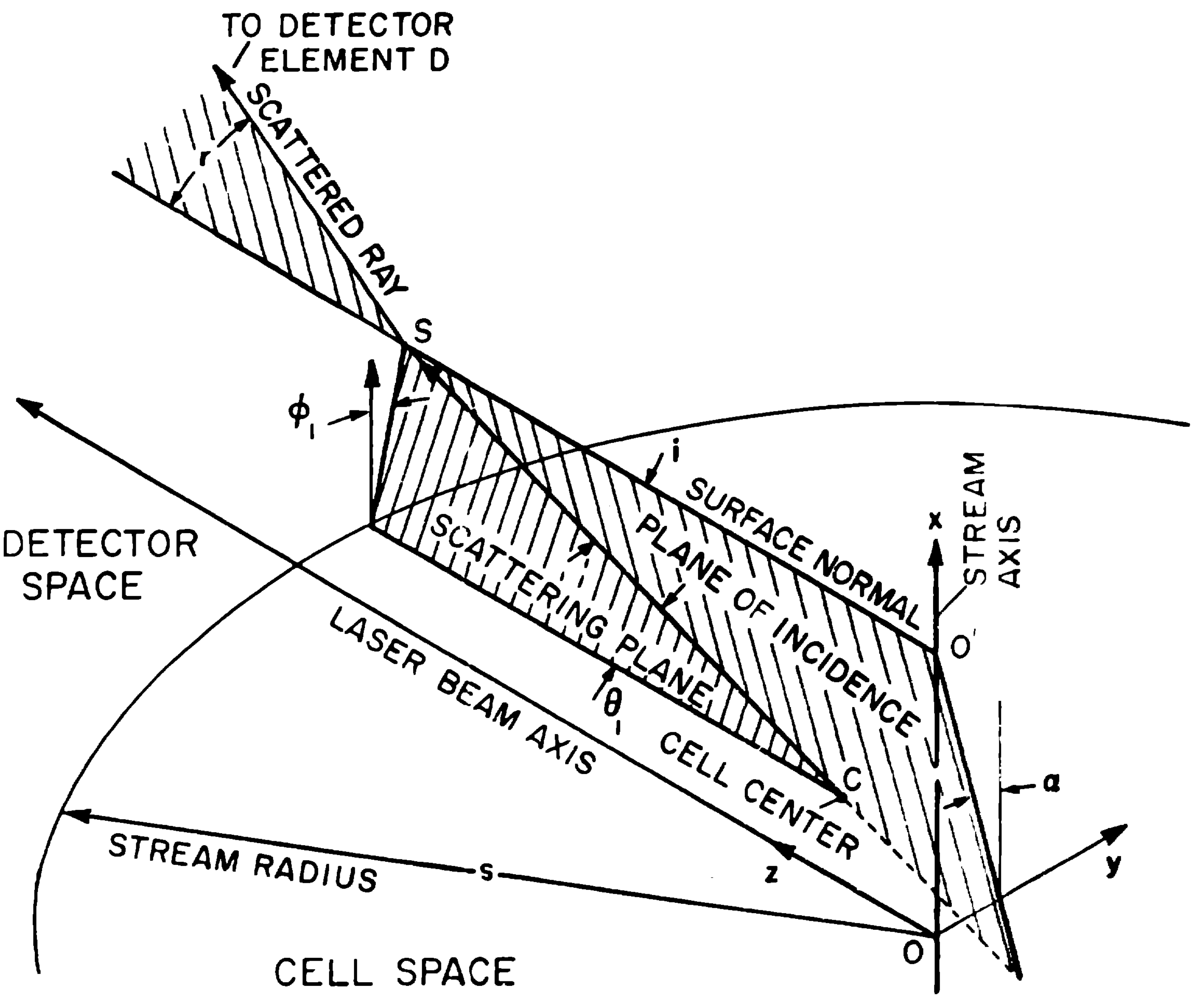
TO DETECTOR
ELEMENT D
SCATTERED RAY
r
S
ϕ_1
i
SURFACE NORMAL
PLANE OF INCIDENCE
SCATTERING PLANE
θ_1
DETECTOR
SPACE
LASER BEAM AXIS
CELL CENTER
C
STREAM
AXIS
x
O'
a
y
z
STREAM RADIUS
s
O
CELL SPACE

FIG. 3. Refractive index effects: Theoretical forward scatter detector response as a function of homogeneous sphere diameter for three different particle relative refractive indices, m. Experimental data points are for polystyrene latex microspheres whose properties are given in Table II. (A) FACS-II, and (B) TPS-1.

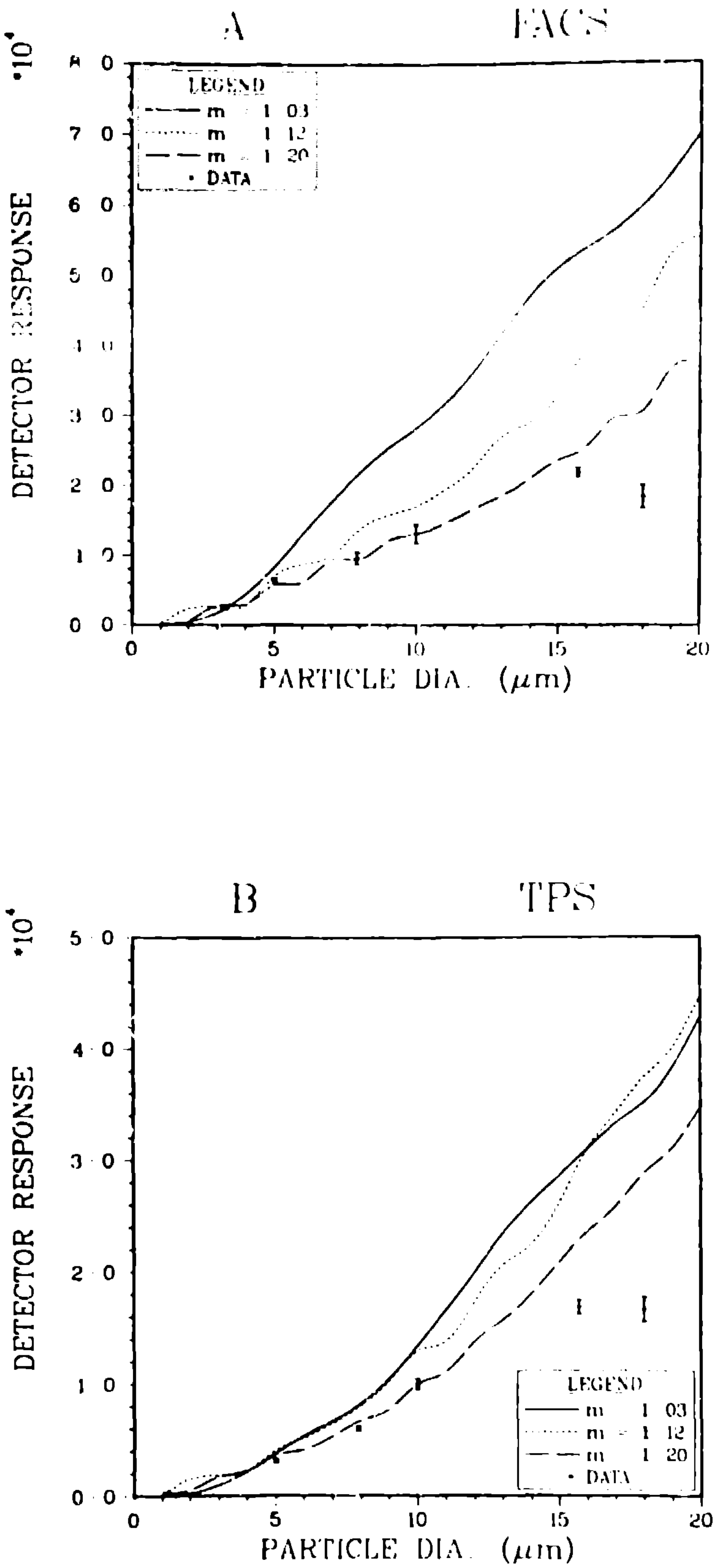
A
FACS
*10⁴
DETECTOR RESPONSE
PARTICLE DIA. (μm)
LEGEND
m = 1.03
m = 1.12
m = 1.20
• DATA
B
TPS
*10⁴
DETECTOR RESPONSE
PARTICLE DIA. (μm)
LEGEND
m = 1.03
m = 1.12
m = 1.20
• DATA

FIG. 4. Position effects: The calculated effects of particle position, C, on the forward scatter detector response vs particle diameter curves for the FACS-II and TPS-1 cell sorters for two particle relative refractive indices. The particle coordinates (X_C, Y_C, Z_C) are given in μm in the legend. (A) FACS-II, m = 1.03; (B) FACS-II, m = 1.20; (C) TPS-1, m = 1.03; and (D) TPS-1, m = 1.20.

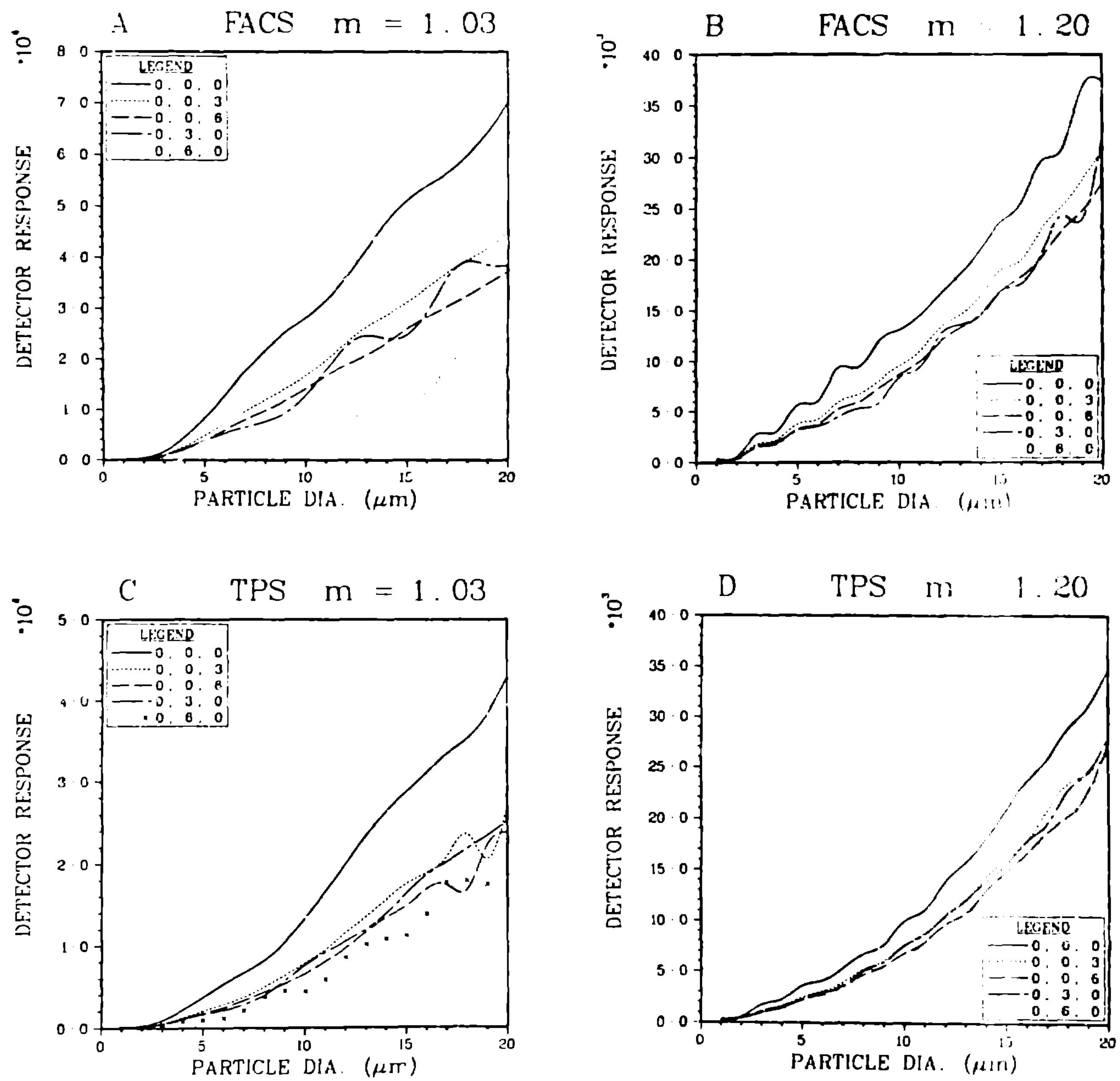

A FACS m = 1.03
B FACS m = 1.20
C TPS m = 1.03
D TPS m 1.20
DETECTOR RESPONSE
PARTICLE DIA. (μm)
LEGEND
0. 0. 0
0. 0. 3
0. 0. 6
0. 3. 0
0. 6. 0

FIG. 5. Comparison between experimental and theoretical forward scatter intensity frequency histograms for 10-μm diameter homogeneous plastic microspheres. Calculated distributions were obtained by choosing a particle at random from a normally distributed Coulter volume distribution (volume coefficient of variation 2%) and placing the particle in the Y-Z plane in the cell stream at random within a normal distribution with the standard deviations given in the legend.

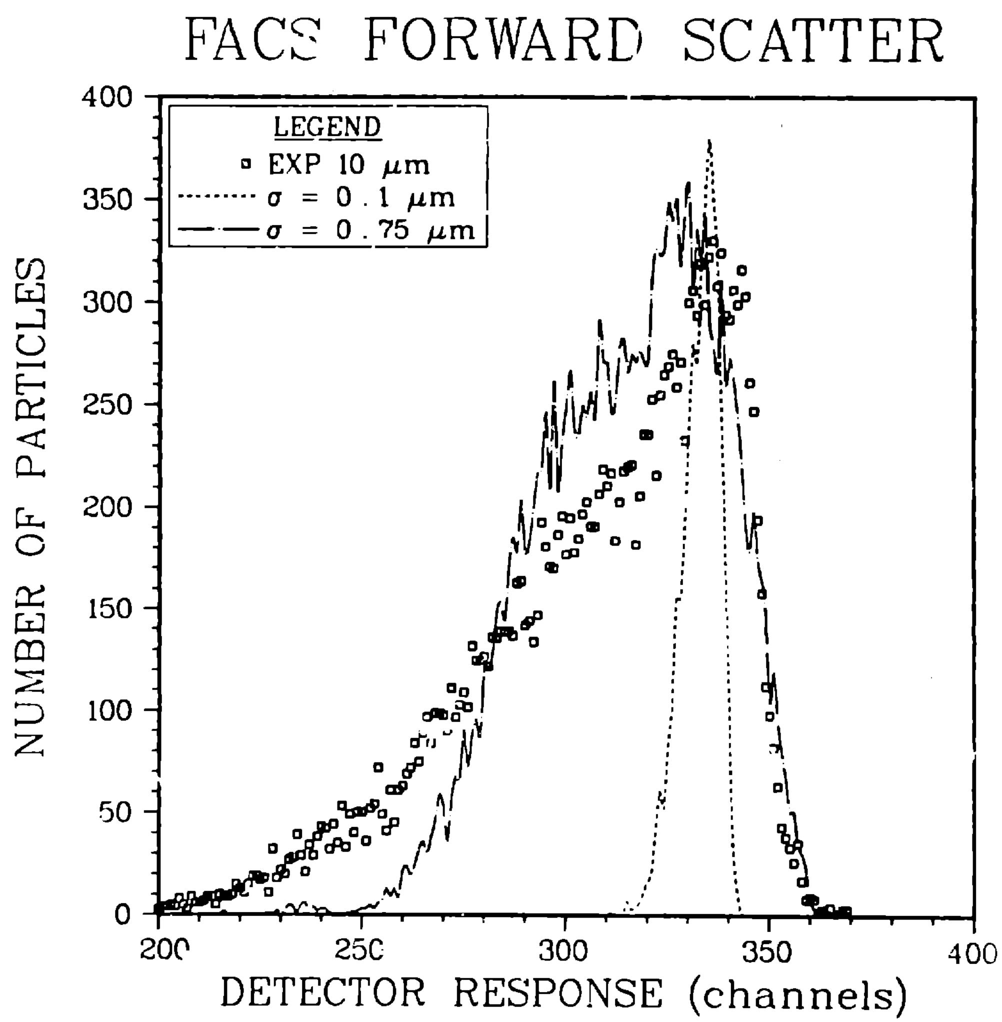
FACS FORWARD SCATTER
LEGEND
EXP 10 μm
σ = 0.1 μm
σ = 0.75 μm
NUMBER OF PARTICLES
0
50
100
150
200
250
300
350
400
200
250
300
350
400
DETECTOR RESPONSE (channels)

FIG. 6. Theoretical 90° FACS-II scatter detector response as a function of homogeneous sphere diameter for three particle relative refractive indices, n. Experimental data points are for uniform polystyrene latex microspheres whose properties are given in Table II.

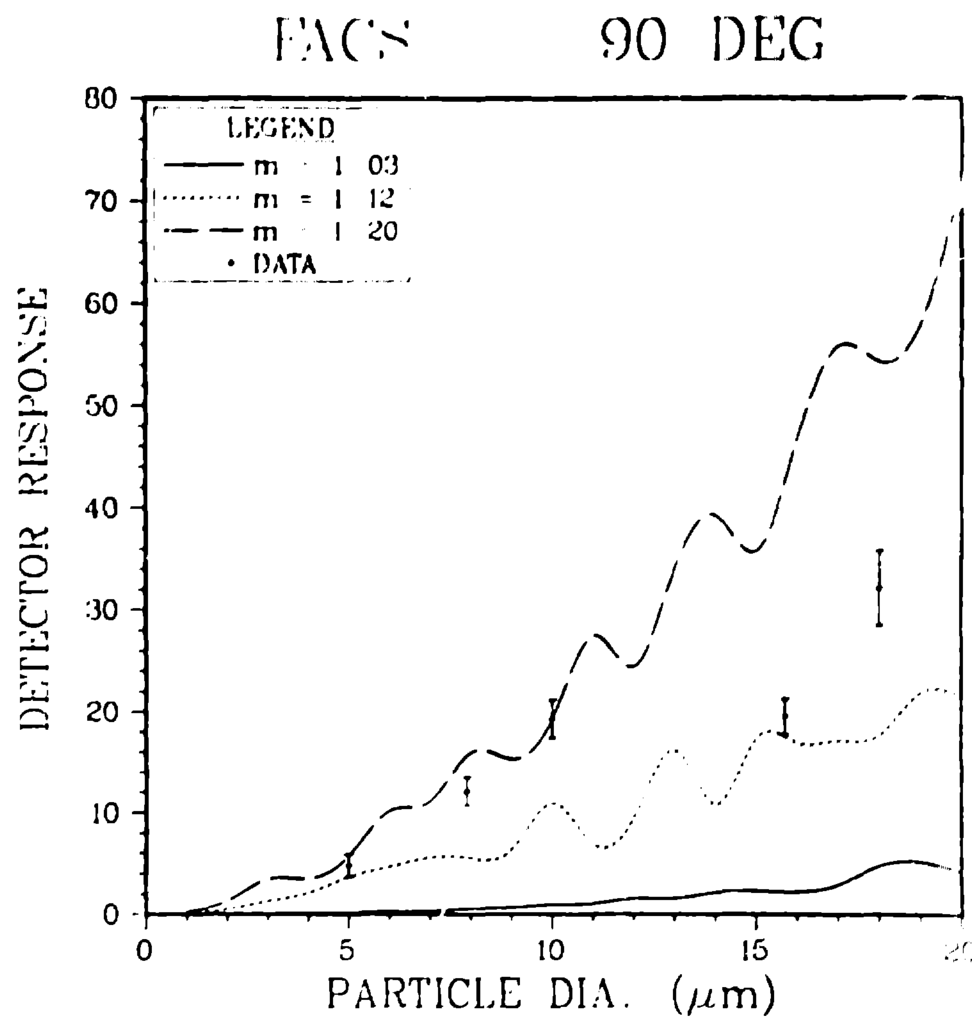

FACS 90 DEG
LEGEND
m 1 03
m = 1 12
m 1 20
DATA
DETECTOR RESPONSE
PARTICLE DIA. (μm)
0
10
20
30
40
50
60
70
80
5
15

FIG. 7. The calculated effects of particle position, C, on the 90° FACS-II scatter detector response for two particle relative refractive indices, m. The particle coordinates (X_C, Y_C, Z_C) are given in μm in the legend. (A) FACS-II, m = 1.03; and (B) FACS-II, m = 1.20.

A FACS90 m 1 . 05

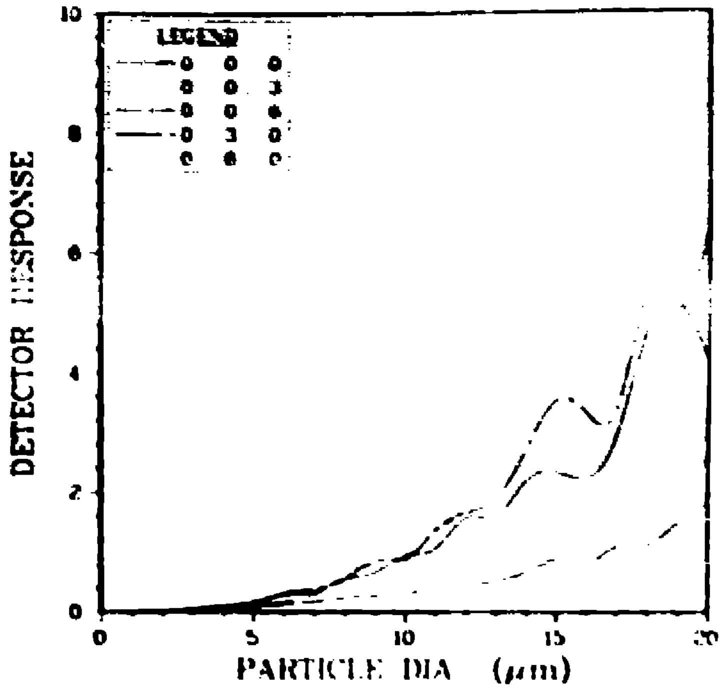

B FACS90 m 1 . 20